

A True Power Detector for RF PA Built-In Calibration and Testing

Pedro Fonseca da Mota
INESC Porto, Faculdade de Engenharia
Universidade do Porto
Porto, Portugal
dee05001@fe.up.pt

José Machado da Silva
INESC Porto, Faculdade de Engenharia
Universidade do Porto
Porto, Portugal
jms@fe.up.pt

Abstract — Different built-in self testing schemes for RF circuits have been developed resorting to peak voltage detectors. These are simple to implement but provide a conditional RF power measurement accuracy as impedance is assumed to be known. A true power detector is presented which allows obtaining more accurate measurements, namely as far as output load variations are concerned. The theoretical fundamentals underlining the power detector operating principle are presented and simulation and experimental results obtained with a prototype chip are described which confirm the benefits of measuring true power, comparing to output peak voltage, when observing output load matching deviations and complex waveforms.

Keywords-RF testing; power amplifier; power sensor

I. INTRODUCTION

The progress currently attained with sub-micron CMOS technologies allows not only to fully integrate RF transceivers on a single substrate, but also to integrate these with the baseband (BB) processing and human interface functions [1]. Testing these circuits, both at production and later in the field, requires usually the measurement of complex parameters, typically resorting to lengthy and expensive test operations and instruments. The cost of testing next generation RF devices is likely to double current figures [1,2].

Different built-in test solutions have been developed to circumvent the embedded RF testing issue [3-8], which allow for replacing functional tests for cheaper and faster operations, yet efficient on detecting defects at the production stage.

Besides testing, on-line monitoring and field maintenance calibration for optimum performance also significantly benefit from the availability of built-in detectors and auxiliary circuits, namely to detect faults and compensate for functional deviations. For example, the BIST scheme proposed in [6] to measure different RF parameters, allows both detecting faults and the automatic performance calibration of a LNA.

In fact, performance degradation can occur due to aging mechanisms and short channel effects, such as time dependent dielectric breakdown (TDDB), hot-carrier injection, metal electromigration, junction breakdown, drain induced barrier lowering (DIBL), and punchthrough [10,12], which are responsible for reliability issues and changing of transistors characteristics. These mechanisms are triggered by high

junctions' peak currents and voltages but depend also on temperature as well as v_{DS} and i_{DS} RMS values.

With complex modulations such as orthogonal frequency division multiplexing (OFDM), the average efficiency of an RF power amplifier (PA) can be relatively low as its output power is most of the time several dB below its peak [12], leading to transistors operating with large DC bias current when the waveform signal power distribution is concentrated in lower levels - i.e., a high crest factor (CF). Consequently, the higher the dissipated power and thermal stress, the higher the probability of inducing a hard breakdown event [13].

Previously proposed BIST circuits often rely in diode based power detectors for the in-circuit observation of RF signals. There are, mainly, four types of power detectors for RF and microwave frequencies: diode, logarithmic, true RMS, and thermal sensors [14-17]. All of them provide indirect power measurements. Diodes can be used as envelope detectors or to compute a signals' power. The power of low amplitude signals can be obtained resorting to the square-law part characteristic of a biased diode or MOS transistor. The observation of voltage's RMS value is usually more useful than peak detection because RMS power is a consistent and standard way to measure and compare dynamic signals regardless their waveform shape. Logarithmic RMS detectors provide a larger dynamic measurement range but their accuracy still depends on signals' waveform envelope and CF. On the other hand, true RMS detectors combine large dynamic range and independence of waveform shape but typically show longer time constants, comparing to diodes. Thermal sensors, namely thermistors and thermocouples, provide wide bandwidth but their usefulness is limited due to their too long time constants and tend to be bulky.

However, observing voltage (or current) only represents power in an indirect way as actual power is estimated by assuming that the load resistance is known $\left(P = \frac{V_{RMS}^2}{R_L}\right)$. As

seen above, cases exist where it is more realistic and efficient, as far as knowing a PA's behaviour is concerned, to observe actual power rather than voltage.

The true power sensor presented herein was developed with the purpose of providing a built-in direct observation of a PA's output power regardless of, under acceptable operating conditions, load value and waveform shape. The remaining of

the paper presents in section II a comparison between observing output voltage and power for evaluating an amplifier's performance. Section III describes the true power detector being proposed. This detector was implemented in a prototype chip in order to evaluate its performance and the validity of the information it provides comparing to that provided by peak detectors. Preliminary experimental results are presented in Section IV. Section V highlights the main conclusions.

II. POWER VS. VOLTAGE MEASUREMENT

Power measurements are critical in RF and microwave systems in both cost and technical terms and are required to be accurate, repeatable, traceable, and convenient. Some specific operating conditions have to be analysed to determine whether power or voltage should be observed.

Within digital communication systems, power level monitoring is needed to ensure that it is high enough to maintain an operating link, while not too high to avoid interference [12], as well as to optimize transmitters' efficiency and signal integrity (e.g., preventing peaking or compression) and receivers' sensitivity and selectivity. The power delivered to the antenna needs to be regulated to compensate for drifts due to, e.g., temperature, components aging and load variations, or as a means to improve efficiency.

When designing a PA its load impedance is matched and adapted in order to maximize the power transferred to the antenna. The actual impedance seen by a well performing PA may actually be not the optimum resistive designed value, as a reactive part is required at the current source [11] and/or introduced by load deviations and parasitics.

Fig. 1 shows the locus of the operating point (i_{DS} vs. v_{DS}) seen by the transistor of a class A PA in the nominal case (N) and when changes of the load reflection coefficient occur: $|\Gamma_N|=0$, $|\Gamma_1|=0.13$, and $|\Gamma_2|=0.1$. It can be seen that, comparing to nominal, the power dissipated in the transistor increases for the Γ_1 case and decreases for the Γ_2 one. However, the v_{DS} peak shows an opposite variation. If one estimated power from $P = \frac{V_{pk}^2}{2R_L}$, not knowing that a variation had occurred in the load resistance, a wrong power would be estimated. In case of a load phase mismatch this difference could be more pronounced.

On the other hand, observing power (or even the true RMS value) does not provide information on asymmetries in positive and negative peak values of the voltage waveforms, such as that observed in Fig. 1 for the Γ_2 case – this is related to the generation of 2nd-order harmonics commonly generated by power amplifiers. This requires that both positive and negative peak detectors are used in order to get a full and correct characterization. When observing voltage, unless one operates in the linear region and with well known waveforms, peak amplitudes may also provide incorrect information.

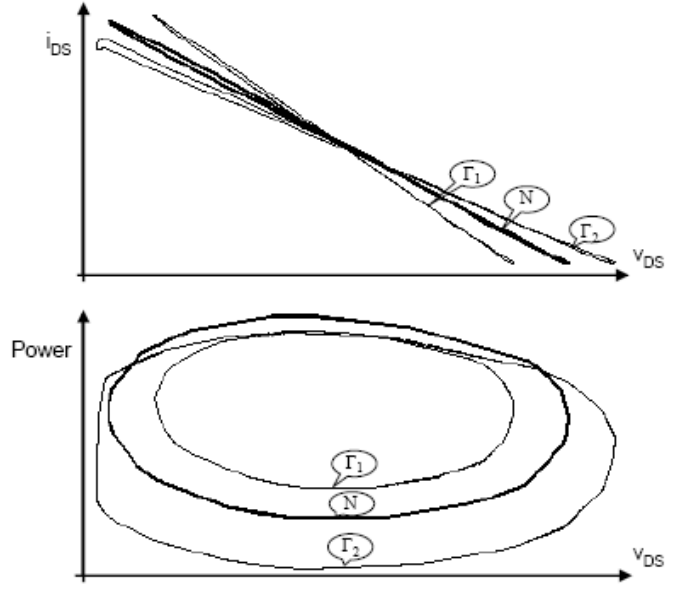


Figure 1 – Locus of (i_{DS}, v_{DS}) and (power, v_{DS}) points of a class A power amplifier.

The presence of an n^{th} harmonic with amplitude A causes a fractional error in the output voltage measurement of, in the worst case, A (n odd) or $n^2 A^2/2$ (n even), and twice these values in the output power measurement [15]. These considerations lead one to conclude that both true power and voltage detectors should be used to ensure full and accurate observation of a PA's behaviour.

III. POWER DETECTOR

It has been shown that the cross-correlation between a circuit's voltage and current signals provides the active power when correlation time delay τ is null, i. e., considering sinewave signals with a θ phase difference,

$$\Re\{v(t) \times i(t)\} = \frac{1}{2} VI \cos(\theta) =$$

$$P = \frac{1}{T} \int_0^T v(t) \times i(t) dt = \frac{1}{2} (V \times I) \times \cos(\theta) \quad (1)$$

If voltage and current present different tones, the correlation result also includes the power due to intermodulation frequencies. Consider that an amplifier's output voltage and current can be represented by polynomials (2) and (3), respectively,

$$v(x) = a_3 \cdot x^3 + a_2 \cdot x^2 + a_1 \cdot x \quad (2)$$

$$i(x) = b_3 \cdot x^3 + b_2 \cdot x^2 + b_1 \cdot x \quad (3)$$

If a two tone input $x = A \cdot \cos(\omega_1) + A \cdot \cos(\omega_2)$ is applied, multiples of the fundamental frequencies, as well as intermodulation products, are generated due to the non-linear transfer characteristic.

The output voltage and current are then given by

$$V(\omega) = k_1 \cdot (\cos(\omega_1) + \cos(\omega_2)) + k_2 \cdot (\cos(2 \cdot \omega_1) + \cos(2 \cdot \omega_2)) + \dots + k_3 \cdot (\cos(3 \cdot \omega_1) + \cos(3 \cdot \omega_2)) + k_4 \cdot (\cos(\omega_1 - \omega_2) + \cos(\omega_1 + \omega_2)) + \dots + k_5 \cdot (\cos(2 \cdot \omega_1 - \omega_2) + \cos(2 \cdot \omega_1 + \omega_2) + \cos(2 \cdot \omega_2 - \omega_1) + \cos(2 \cdot \omega_2 + \omega_1)) \quad (4)$$

$$I(\omega) = m_1 \cdot (\cos(\omega_1) + \cos(\omega_2)) + m_2 \cdot (\cos(2 \cdot \omega_1) + \cos(2 \cdot \omega_2)) + \dots + m_3 \cdot (\cos(3 \cdot \omega_1) + \cos(3 \cdot \omega_2)) + m_4 \cdot (\cos(\omega_1 - \omega_2) + \cos(\omega_1 + \omega_2)) + \dots + m_5 \cdot (\cos(2 \cdot \omega_1 - \omega_2) + \cos(2 \cdot \omega_1 + \omega_2) + \cos(2 \cdot \omega_2 - \omega_1) + \cos(2 \cdot \omega_2 + \omega_1)) \quad (5)$$

where coefficients k_i and m_i depend on amplitude A and coefficients a_i and b_i , respectively. After the multiplication of voltage and current signals, the DC terms, i. e., average power, returns also the contribution of the power of other tone components besides the fundamentals, as

$$P_{avg} = k_1 \cdot m_1 + k_2 \cdot m_2 + k_3 \cdot m_3 + k_4 \cdot m_4 + 2 \cdot k_5 \cdot m_5 \quad (6)$$

A power detector was developed based on this principle (Fig. 2). The correlator is made of a mixer whose, inputs are obtained from the current and voltage signals to be considered, followed by a simple low-pass filter.

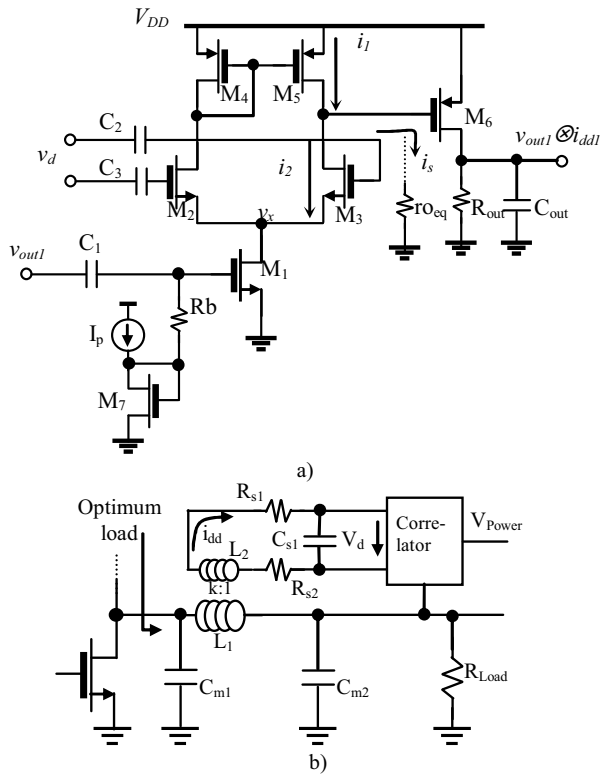


Figure 2 – a) Correlator circuit; b) Power detector.

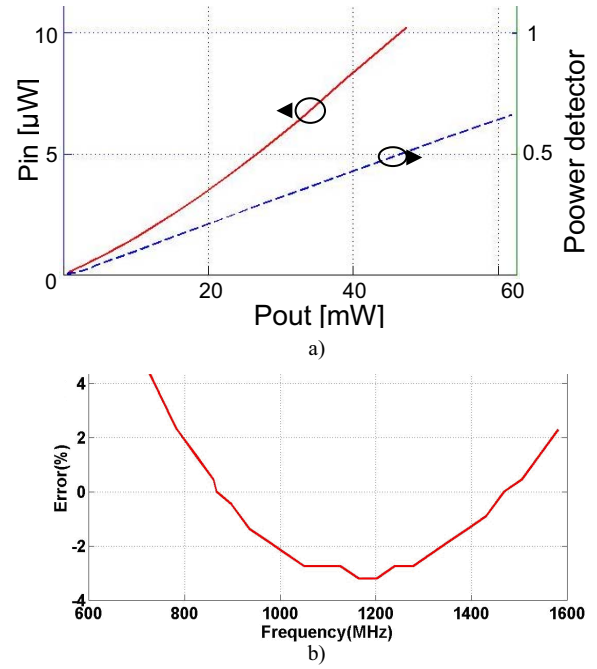


Figure 3 – a) Power detector transfer characteristic at nominal frequency, b) Variation of measurement error with frequency.

The mixer's input differential voltage v_d (which is proportional to the PA's output current) is obtained with a coreless transformer whose primary inductance makes also part of the PA's output impedance matching network (Fig 2.b).

Fig 3.a) shows the simulated power detector transfer characteristic (dashed line) and figure 3.b) the measurement error as a function of frequency – Fig. 3.a) shows also the characteristic (solid line) of the PA to be presented in section IV. It can be seen that good measurement linearity is obtained in a relatively large bandwidth – the detector bandwidth is centered at 866 MHz. This allows obtaining a true power measurement for different voltage waveforms.

Fig. 4 shows the transfer characteristics obtained with sine and square waveforms, revealing that a good linearity is obtained in both cases. For the square-wave case the power measurement error varies from -7%, for the lower amplitudes, to -4% for the higher amplitudes.

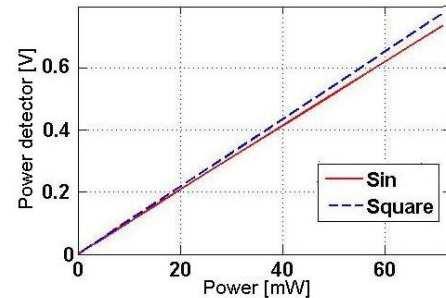


Figure 4 – Power detector transfer characteristics for sine and square waveforms.

IV. DEMONSTRATION PROTOTYPE

A prototype demonstration chip was designed and fabricated in a CMOS 0.35 μm technology. It implements an 866 MHz class AB power amplifier ($P_{\text{max}} = 19 \text{ dBm}$, $\text{Gain} = 15 \text{ dBm}$), whose characteristic is the solid line shown in Fig. 3.a), a pre-amplifier, the power detector, as well as peak voltage detectors (Fig. 5.a). The pre-amplifier is a digitally controlled variable gain amplifier usually employed to control PA's output power, but that for testing purposes can also be used to generate different amplitude testing stimuli.

Fig. 5.b) shows the photo of the prototype chip. The area of the cross-correlator ($80 \times 80 \mu\text{m}^2$ square in Fig. 5.b) is mostly occupied by capacitors and bias resistors. Nevertheless, this area is smaller than 10% the total chip area (inductors included) representing thus a reduced area overhead. The transformer does not imply any area overhead as that is imposed by the primary winding which makes part of the matching network.

In order to implement an accurate and linear peak voltage detector the scheme (Fig. 6.a) proposed in [16] was adopted. It comprises two simple detectors (Fig. 6.b), being the final peak detector output voltage obtained from the sum of one of them with a scaled value of the difference between the two ($V_{\text{out}} = V_{d1} + N(V_{d2} - V_{d1})$).

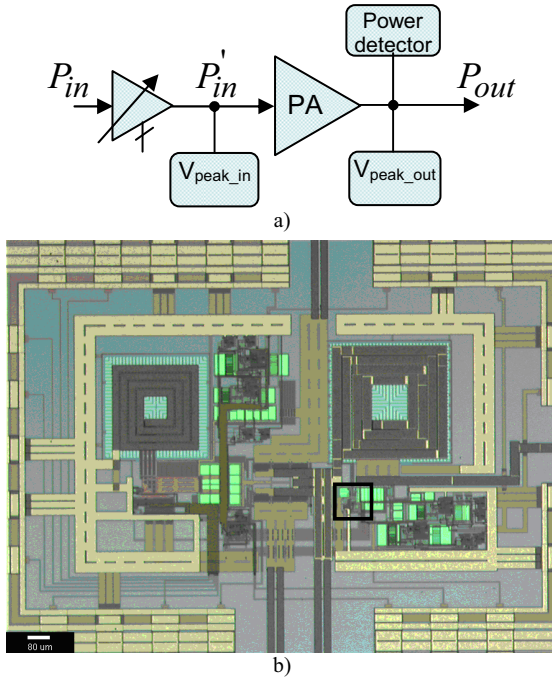


Figure 5 – Prototype chip. a) Block diagram , b) Chip photograph.

The voltage detectors were calibrated in order to provide a linear response to the output peak voltage for the nominal load response. The transfer characteristics shown in Fig. 7 show that good measurement linearity is obtained. However, as the detector is optimized for narrowband response, the squarewave

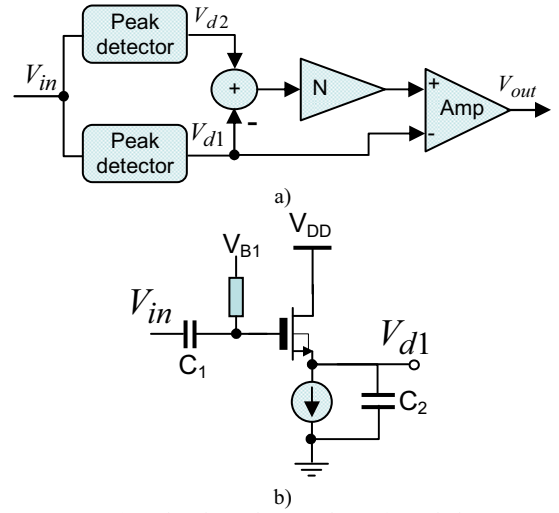


Figure 6 – a) Peak voltage detector; b) Basic peak detector.

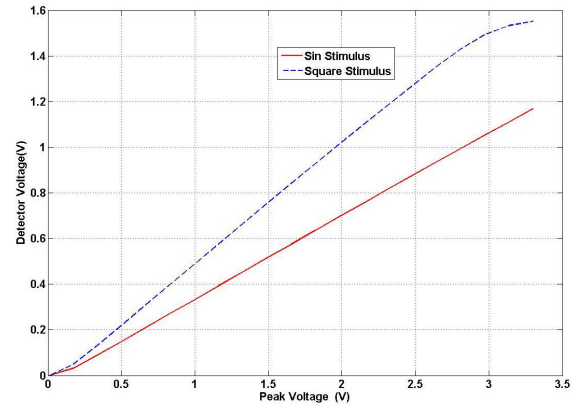


Figure 7 – Simulated peak voltage detector transfer characteristics.

response overestimates signal's amplitude as it provides actually that of the fundamental component.

Preliminary lab measurements were obtained with this chip that confirm the correct operation of the two sensors, as well as that more correct information on the power delivered to the load can be obtained when observing power comparing to that obtained from voltage.

The curves depicted in Fig. 8 show the measured transfer characteristics of the two sensors. It can be seen that the power sensor shows better linearity up to about 7 mW (error $< 0.5 \text{ dB}$) and that the peak detector shows better performance for the higher powers. Due to matching issues these measurements were performed at a frequency lower than nominal.

Other measurements were carried-out to evaluate the effect of PA's load variations. Fig. 9 shows three cases of load variations with reflections coefficients of: a) $\Gamma=0.33$ resistive; b) $\Gamma=0.98$ inductive; and c) $\Gamma=0.2$ capacitive. It can be seen that in all three cases the power obtained with the power sensor is closer to the expected one.

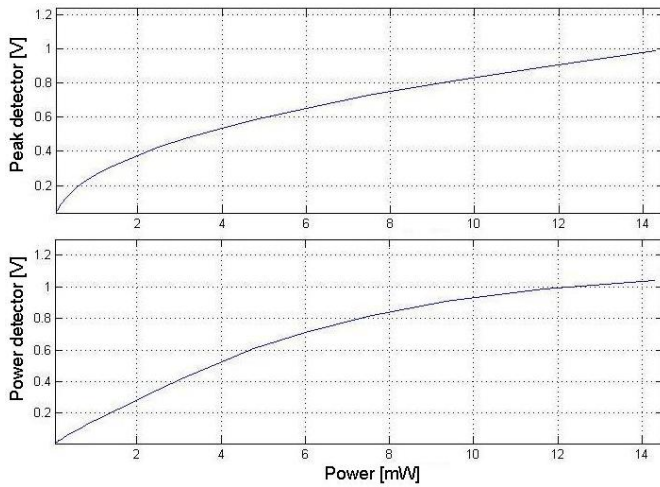


Figure 8 – Measured peak voltage and power detectors transfer characteristics.

The power estimated with the peak voltage detector is different as its response is calibrated for the nominal optimum load resistance, i. e., power ($P = \frac{V_{pk}^2}{2R_L}$) is computed using the expected load resistance value and not the actual one. New measurements will be carried-out after new matching and parasitics de-embedding procedures.

In order to evaluate power observation with different waveforms, measurements were performed within single-tone and multi-tone signals, maintaining the same total power (fundamental plus harmonics) at the PA output. Fig. 10.a) shows that the power detector provides the same measurement, regardless the signal waveform.

This particularity allows detecting an increase of power even when the PA enters into saturation. Fig. 11 shows the response of both detectors for increasing powers of an IEEE 802.1 OFDM signal. While with the power detector one can observe an increasing power due to the increasing of harmonics amplitudes, the peak detector reflects the tendency to saturation of the output voltage.

V. CONCLUSIONS

The development of built-in self-test solutions for RF circuits has not yet reached the maturity required to allow replacing exhaustive, but time-consuming, characterization testing operations, for tests capable of screening malfunctioning circuits due to processing defects and process variations. Diode based peak voltage detectors have been used in the proposed built-in RF test schemes. Nevertheless, observing voltage does not provide accurate circuits' performance detection namely when impedance matching variations occur. Being PAs the most challenging circuits as far as integration related reliability issues are concerned, it is critical that transistors' behaviour is correctly monitored.

The power sensor presented here provides an alternative means to monitor PA's output power, capable of measuring true

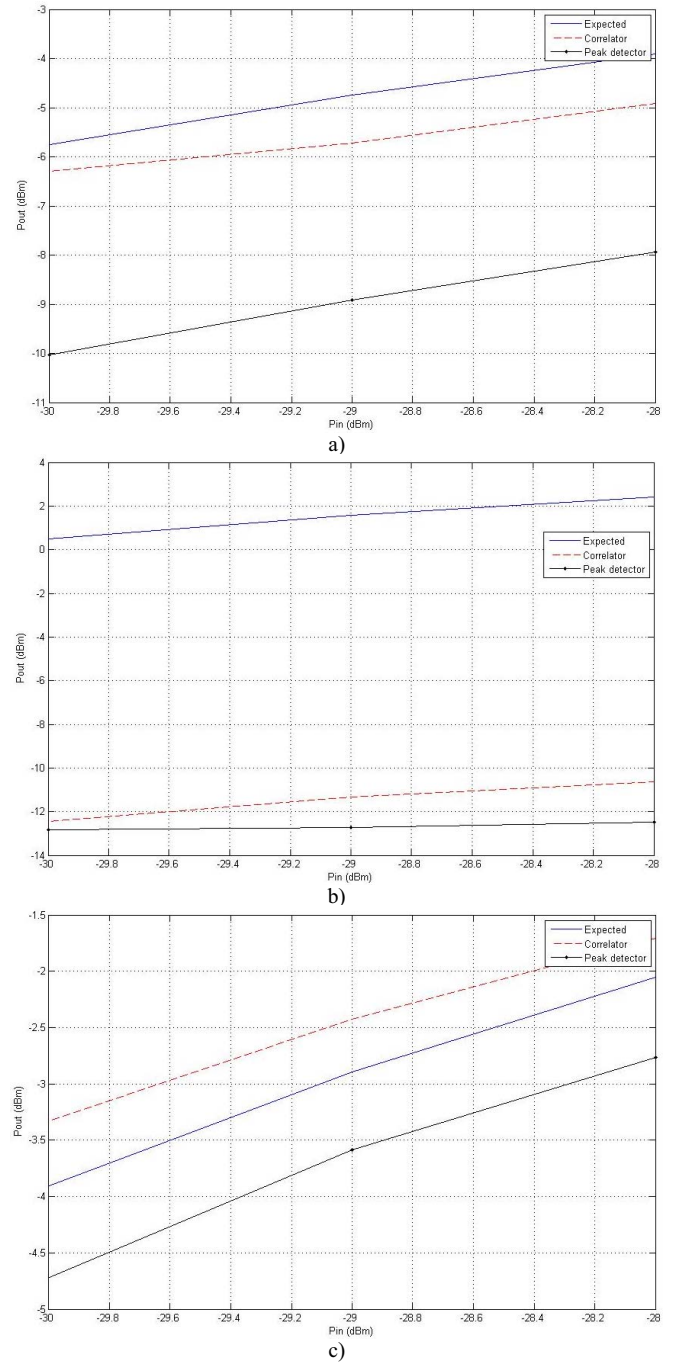


Figure 9 – Voltage and power detectors transfer characteristics obtained.

power and detecting impedance mismatches, as it is shown from the experimental results already obtained with a prototype chip.

Eventually peak voltage and true power sensors can be used together as a means to monitoring signal crest factors. Relying on true power measurements one can implement regulation loops for automatic level control, namely to improve linearity, and correct the PA operation for process, voltage and temperature variations.

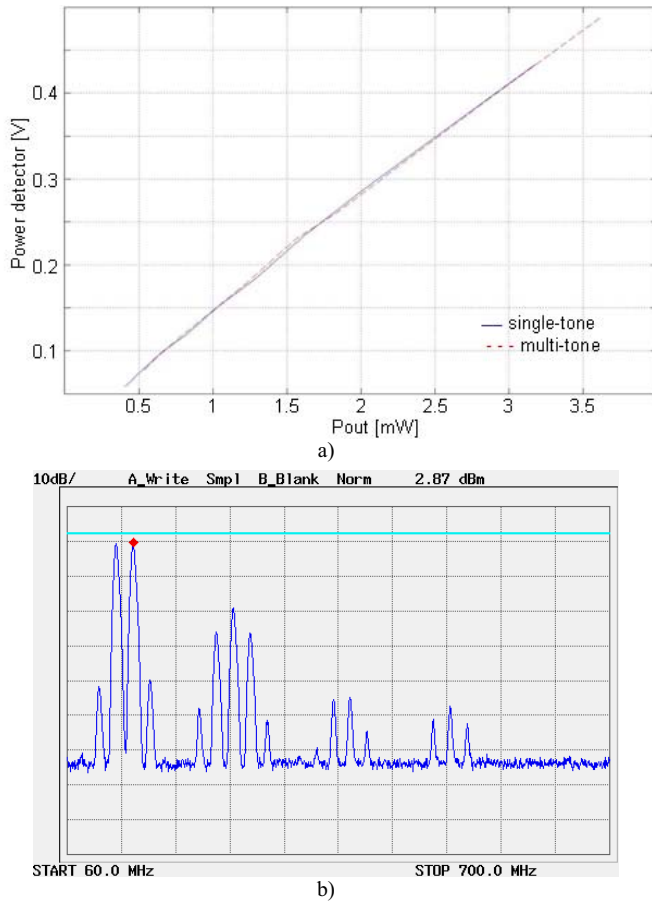


Figure 10 – Response of the power sensor to single-tone and b) multi-tone signals.

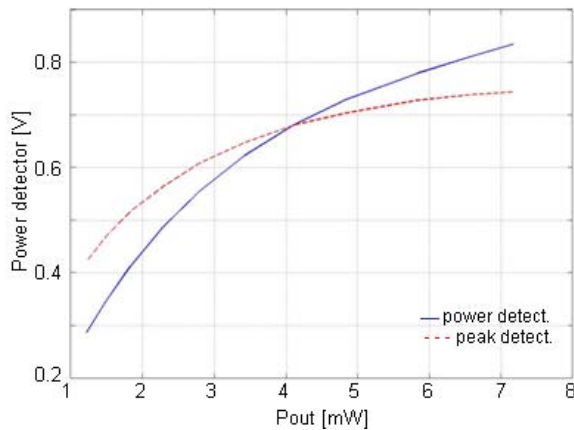


Figure 11 – Response of the power sensor to an OFDM signal within PA's golden and defective cases.

ACKNOWLEDGMENT

The authors are thankful to Me. Ricardo Veiga who collaborated in the development of the prototype chip. This work has been carried-out in the framework of project EDAM-SenseCardioHealth with the support of programme MIT|Portugal, grant MIT-Pt/EDAM-EMD/0007/2008, and project Eureka/Catrene TOETS CT302.

REFERENCES

- [1] W.Y. Lau, "Measurement challenges for on-wafer RF-SOC test," Proc. of the 27th IEEE/SEMI Int. Electronics Manufacturing Technology Symp., pp. 353-359, July 2002.
- [2] Ken Harvey, Next-generation RF devices impact test, *EE-Evaluation Engineering*, Oct. 2007.
- [3] R. Green and J. Janesch. The Importance of fast, economical testing for RFIC PAs, Mobile Phones. *RF Design Magazine*, Jun. 2004, pages 20–26.
- [4] D. Lupea, U. Pursche, and H. J. Jentschel. Spectral signature analysis BIST for RF front-ends. *Journal of Advances in Radio Science*, 2003, 1:155–160.
- [5] M. Negreiros, L. Carro, and A.A. Susin, "Low cost analog testing of RF signal paths". Proc. of IEEE Design Automation and Test in Europe, pp. 292–297, Feb. 2004.
- [6] J.-Y. Ryu, B. C. Kim, and I. Sylla, "A new low-cost RF built-in self-test measurement for system-on-chip transceivers", IEEE Trans. on Instrumentation and Measurement, Vol. 55, No. 2, Apr. 2006, pp. 381 – 388.
- [7] R.Voorakaranam, S.S. Akbay, S. Bhattacharya, S. Cherubal, A. Chatterjee, "Signature testing of analog and RF circuits: algorithms and methodology", IEEE Trans. on Circuits and Systems I, Vol. 54, No. 5, May 2007, pp. 1018–1031.
- [8] H.-G. Stratigopoulos, Jean Tongbong, S. Mir, "A general method to evaluate RF BIST techniques based on non-parametric density estimation", Proc. of IEEE Design, Automation and Test in Europe, 2008.
- [9] B. El Kassir, C. Kelma, B. Jarry, M. Campovecchio, "Built-in self test for error vector magnitude measurement of RF transceiver", Proc. of International Test Conference, 2009.
- [10] M.A. Alam, B.E. Weir, P.J. Silverman, Y. Ma, and D. Hwang, "The statistical distribution of percolation resistance as a probe into the mechanics of ultra-thin oxide breakdown," Proc. of the Int. Electron Devices Meeting, pp. 529-532, 2000.
- [11] P. Colantonio, F. Giannini, E. Limiti, A. Ticconi, "Prediction of PA optimum load by small signal parameters", Int. Workshop on Integrated Nonlinear Microwave and Millimeter-Wave Circuits, pp. 183 – 186, Aveiro, Jan. 2006.
- [12] Mark Ruberto, Ofir Degani, Shay Wail, Alex Tender, Amir Fridman, Gennady Goltman, "A reliability-aware RF power amplifier design for CMOS radio chip integration", IEEE 46th Int. Reliability Physics Symp., pp. 536-540, 2008.
- [13] M.A. Belaïd, K. Ketata, K. Mourgues, H. Maanane, M. Masmoudi, J. Marcon, "Comparative analysis of accelerated ageing effects on power RF LDMOS reliability", *Microelectronics and Reliability*, Vol. 45, No. 9-11, Sep. 2005, pp. 1732-1737.
- [14] Nathan O. Sokal, A. D. Sokal, "Accurate measurement of RF power amplifier efficiency and power output without and RF power meter", IEEE Journal of Solid-State Circuits, Vol. SC-12, No. 5, Oct. 1977.
- [15] J.C. Cowles, "The evolution of integrated RF power measurement and control", IEEE MELECON 2004, Dubrovnik, May 12-15, 2004.
- [16] C. Presti, F. Carrara, A. Scuderi, and G. Palmisano, "Fast peak detector with improved accuracy and linearity for high-frequency waveform processing", IEEE Intl. Symp. on Circuits and Systems, pp. 3884–3887, 2007.
- [17] Agilent Fundamentals of RF and Microwave Power Measurements, Application Note 64-1C.